Controlling polariton dispersion in anisotropic media via isotopic enrichment

Thiago S. Arnaud[1], Mingze He[1], Ryan Spangler[2], Joshua D. Caldwell[1]

[1]*Department of Mechanical Engineering, Vanderbilt University, Nashville, TN*, [2]*Department of Materials Science and Engineering Pennsylvania State University, State College, PA*

Background

$$\text{Diffraction Limit}\quad d = \frac{\lambda}{2sin\theta}$$

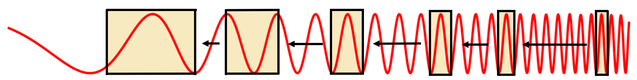

Radiation Type	Radio	Microwave	Infrared	Visible	Ultraviolet	X-ray	Gamma ray
Wavelength / m	10^{3}	10^{-2}	10^{-5}	0.5×10^{-6}	10^{-8}	10^{-10}	10^{-12}

- Polaritons are quasiparticles of light coupled a form of matter
- The intrinsic material properties dictate the class of polaritons supported

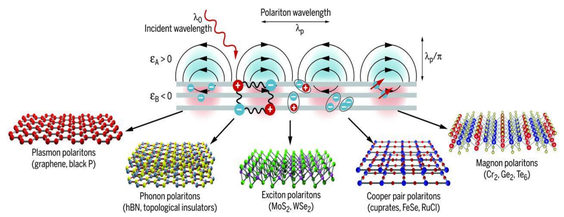

Figure 1: *General classifications of polaritons.*[1]

Hyperbolic Materials

- The Reststrahalen band (RB) is the spectral region that supports polaritons where the real-valued permittivity is negative.
- Hyperbolic materials have a permittivity tensor with different in and out-of-plane permittivities.
- α-MoO_3 exhibits in-plane anisotropy, leading to three RBs where hyperbolic phonon polaritons (HPhP) are supported.

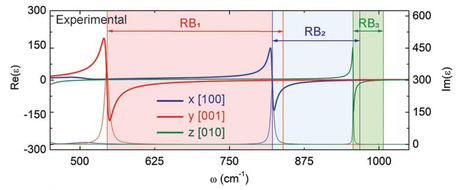

Figure 2: *Infrared dielectric function of MoO_3 with the corresponding direction of HPhP propagation.*[2]

Orthorhombic Molybdenum Trioxide (α-MoO_3)

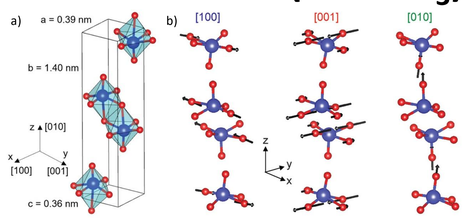

- Normal modes in the unit cell reported in literature.
- Naturally abundant MoO_3 contains seven stable isotopes of significant concentration: ^{92}Mo, ^{94}Mo, ^{96}Mo, ^{98}Mo, and ^{100}Mo.
- HPhPs in ^{xx}Mo enriched samples have been investigated in literature.

Figure 3: ***a)*** *Orthorhombic unit cell crystalline structure of MoO_3.*[2] ***b)*** *Atomic displacements calculated from density functional theory for each RB shown in Fig 2.*[2]

Little is understood on the anisotropic dependence of HPhPs from monoisotopic enriched MoO_3

Monoisotopic enrichment of MoO_3

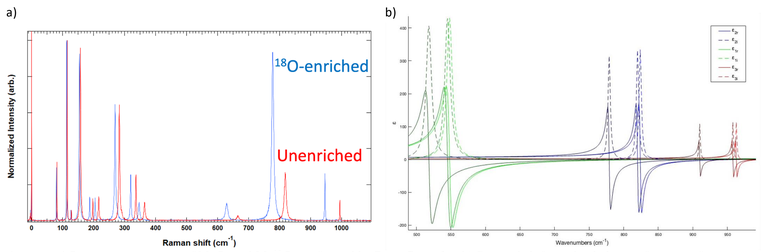

Figure 4: *a) Raman spectroscopy of MoO_3 and $Mo^{18}O_3$ performed by* ***Ryan Spangler****. b) Spectral shifts in the dielectric function of $^{xx}Mo^{xx}O_3$ calculated with the transfer matrix method.*

- 5% redshift is observed in ^{18}O enrichment from Raman.
- Dielectric function is preliminarily calculated by applying the corresponding shift to naturally abundant MoO_3 for each isotope.

Experimental procedure

Sample preparation

Mechanical Exfoliation[3]

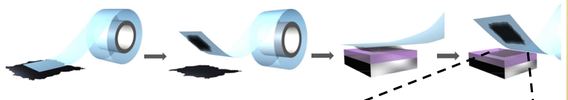

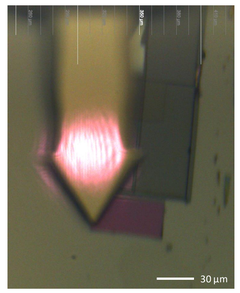

Flake Selection

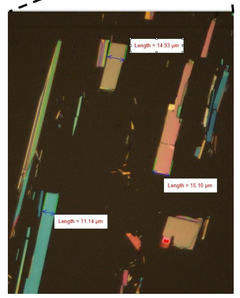

Flakes must be sufficiently wide to avoid Fabry Perrot modes (standing waves of HPhPs from both sides)

150 µm < Flake thickness < 600 µm

Scattering-type scanning near-field optical microscopy (s-SNOM)

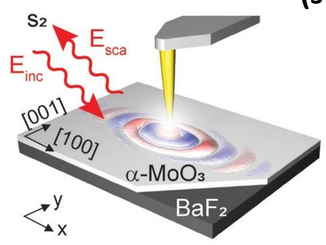

- Quantum cascade laser is scattered off a metallized AFM tip to have sufficient momentum to launch HPhPs.
- The near-field E-field from the HPhP scatters off the tip and collected by the detector.
- Near-field polariton signal is demodulated from the far-field via higher order tip harmonic oscillations.

Figure 5: *Experimental setup of a SNOM system for near-field imaging.*[2]

Polariton Fourier Analysis

Raw SNOM scans

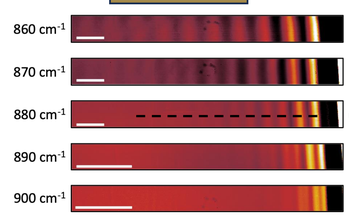

Figure 6: *SNOM images of HPhPs propagating in $Mo^{18}O_3$ along the [100] crystal direction.*

Extracted intensity line scan

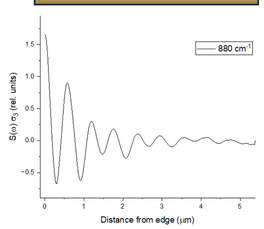

Figure 7: *1-D HPhP line profile with far-field correction*

FFT with Lorentz peak fittings

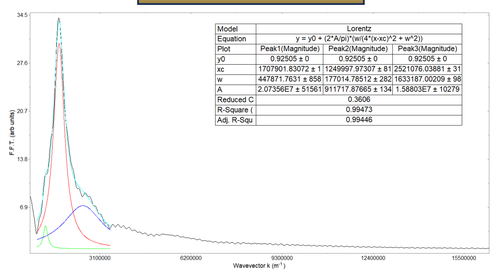

Model	Lorentz		
Equation	y = y0 + (2*A/pi)*(w/(4*(x-xc)^2 + w^2))		
Plot	Peak1(Magnitude)	Peak2(Magnitude)	Peak3(Magnitude)
y0	0.92505 ± 0	0.92505 ± 0	0.92505 ± 0
xc	1707901.83072 ± 1	1249997.97307 ± 81	2521076.03881 ± 31
w	447871.7631 ± 858	177014.78512 ± 282	1633187.00209 ± 98
A	2.07356E7 ± 51561	911717.87665 ± 134	1.58803E7 ± 10279
Reduced C	0.3606		
R-Square (	0.99473		
Adj. R-Squ	0.99446		

- Lorentzian peaks fitted to FFT to discern between tip-launched, edge-launched, or higher order modes.
- Complex polariton wavevector reconstructed: $\tilde{k}_p = \mathbf{k}_p + ik_p$
  - $\mathbf{k}_p$: Peak position
  - k_p: FWHM of peak
- Propagation length: $L_p = \frac{1}{k_p}$

Figure 8: *Fast-Fourier transform from 1-D SNOM line scans with Lorentz peak fits.*

Current Progress

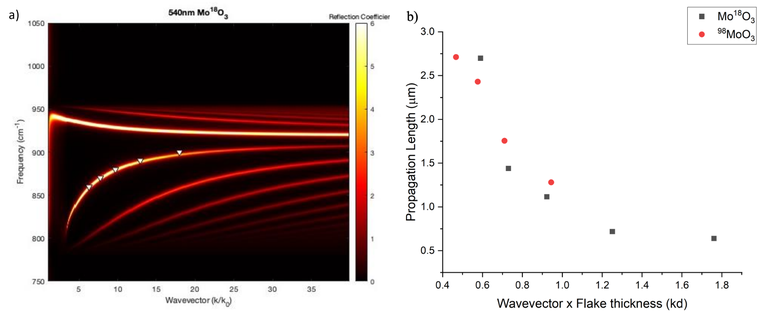

Figure 9: *a) Calculated dispersion of $Mo^{18}O_3$ for the RB_2 and RB_3. White triangle data points are the experimental HPhP wavevectors extracted from SNOM. b) HPhP propagation length for monoisotopic samples. $98MoO_3$ data had been completed by* ***Mingze He****.*

Polariton propagation length in RB_2 shows no discernable impact from ^{18}O enrichment

Ongoing efforts

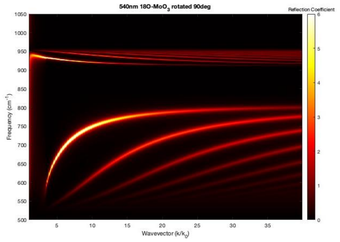

Figure 10: *Dispersion curve for $Mo^{18}O_3$ polarized to support HPhPs in the RB_1.*

- Completing the experimental dispersion mapping for both the RB_1 and RB_3 on each isotope.
- Extend the study with polariton lifetimes, group velocity, and confinement factor.
- Collaborators calculating phonon density of states through DFT to predict atomic contributions in each RB.

Future Work: Monoisotopic heterostructures

Superimposed Branches

Increased Density of States

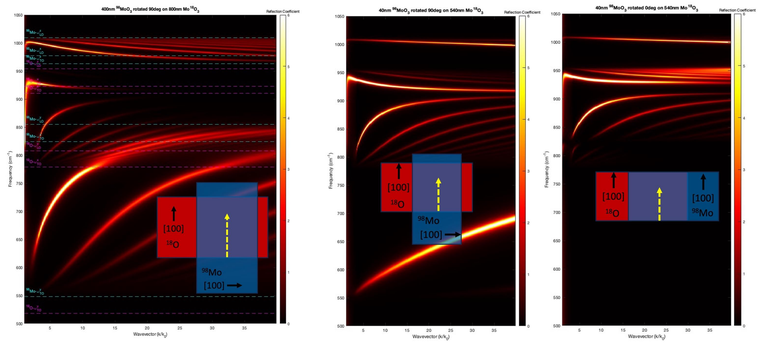

References and Acknowledgements

T.S.A. would like acknowledge VINSE and the Office of Naval Research MURI Grant (No. 301297) for their support. This material is based upon work supported by the National Science Foundation Graduate Research Fellowship Program under Grant No. 2444112. Any opinions, findings, and conclusions or recommendations expressed in this material are those of the author(s) and do not necessarily reflect the views of the National Science Foundation.

[1] Basov, D. N., Fogler, M. M. & García De Abajo, F. J. Polaritons in van der Waals materials. *Science* **354**, aag1992 (2016).

[2] Álvarez-Pérez, G. *et al.* Infrared Permittivity of the Biaxial van der Waals Semiconductor α-MoO $_3$ from Near- and Far-Field Correlative Studies. *Adv. Mater.* **32**, 1908176 (2020).

[3] Liu, X. *et al.* Thin-film electronics based on all-2D van der Waals heterostructures. *J. Inf. Disp.* **22**, 231–245 (2021).